International Journal of Biological Macromolecules 270 (2024) 132493

Contents lists available at ScienceDirect

International Journal of Biological Macromolecules

journal homepage: www.elsevier.com/locate/ijbiomac

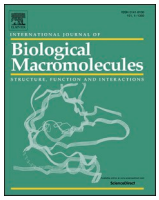

Chitosan for improved encapsulation of thyme aqueous extract in alginate-based microparticles

Giada Diana [a], Alessandro Candiani [a], Alice Picco [a], Andrea Milanesi [a,b], Margherita Stampini [a], Elia Bari [a], Maria Luisa Torre [a,c], Lorena Segale [a,b,*], Lorella Giovannelli [a,b]

[a] Department of Pharmaceutical Sciences, Università del Piemonte Orientale, Largo Donegani 2, 28100 Novara, Italy
[b] APTSol S.r.l., Largo Donegani 2, 28100 Novara, Italy
[c] PharmaExceed, Piazza Castello 19, 27100 Pavia, Italy

ARTICLE INFO

Keywords:
Alginate microparticles
Chitosan
Encapsulation efficiency
Aqueous extract

ABSTRACT

Ionotropic gelation is a low-cost, easy and green microencapsulation technique. However, the encapsulation of highly soluble compounds is challenging because of the wide loss of material into the external water phase by passive diffusion and the consequent low encapsulation efficiency. In this work an important increase of encapsulation efficiency for *Thymus vulgaris* L. aqueous extract in alginate-based microparticles has been obtained. A formulation with the proper thyme extract/alginate ratio (30:70) was used as reference and then optimized by adding different co-carrier excipients. Microparticles obtained by dropping a solution containing thyme extract and alginate into a chitosan/calcium-chloride/acid acetic solution lead to a high encapsulation efficiency (70.43 ± 5.28 %). After drying, microparticles had a particle size of 1096 ± 72 μm, 20.087 ± 1.487 % of extract content, 6.2 % of residual water, and showed a complete release of thyme extract within one hour. Combining alginate and chitosan as polymeric co-carrier was a valuable option for efficiently encapsulating an aqueous extract by ionotropic gelation.

1. Introduction

The delivery of hydrophilic active compounds, like drugs and nutraceuticals, represents a challenge, especially when susceptible to external factors (pH, temperature, and oxygen) responsible for their chemical/biochemical degradation or to the gastro-intestinal processes, which limit and reduce their bioavailability, biological half-life, and tissue uptake [1].

Microencapsulation can help to overcome these drawbacks, providing protection and controlled release of active compounds. In this regard, some strategies are used in the pharmaceutical and nutraceutical fields to get through these problems quickly. One of these is the use of spray drying, which allows the production of powders starting from a liquid system that is atomized in a chamber in which hot air flows. However, the heat and/or, in some cases, organic solvents used to prepare the material to be treated could compromise the active compound. The multiple emulsions, precisely the water-in-oil-in-water emulsions, might seem an alternative, but they are thermodynamically unstable [1]. Another technique recently applied for its several advantages is spray congealing of water-in-oil emulsion to produce solid lipid microparticles [2], an approach based on the solidification of a molten slurry (that in this case is water-in-oil emulsion in which the oily phase is a molten lipid) atomized in an airflow kept at a temperature below the melting point of the lipid. Despite its affordability and the absence of solvents, the criticalities of this production process involve the high temperature required to melt the lipid. Ionotropic gelation, instead, is an excellent option to better preserve the bioactive substances thanks to its mild process conditions and the possibility to select biocompatible, biodegradable, and low-toxic materials as polymeric carriers (for example, sodium alginate). Ionic gelation consists of the dripping of an alginate-drug mixture into a gelling bath rich in bivalent cations (*e.g.*, Ca^{2+}), which link the -COO^- groups of two different polymeric chains, forming a three-dimensional network structure and consequently transforming each liquid drop into gelled microparticle [3]. However, in general, microencapsulation of a highly soluble drug with techniques that require the curing of microparticles into an external water phase is responsible for low entrapment efficiency and loading capacity due to the partitioning of the active substance from polymer droplets to the

* Corresponding author.
E-mail address: lorena.segale@uniupo.it (L. Segale).

https://doi.org/10.1016/j.ijbiomac.2024.132493
Received 23 February 2024; Received in revised form 2 May 2024; Accepted 16 May 2024
Available online 18 May 2024

large volume of the curing aqueous bath [2,3]. For this reason, the treatment *via* ionotropic gelation of formulations loaded with hydrophilic and highly water-soluble compounds is a stiff challenge, as it becomes quite difficult to gain cost-effectiveness if a high quantity of expensive drugs is sacrificed during the microparticle production process. Researchers proposed several strategies to improve the entrapment ability of alginate-based microspheres: a good encapsulation efficiency was obtained by the saturation of the gelling solution with the bioactive substance often matched with the variation of the calcium chloride concentration in the gelling bath, and the addition of different types of filler into the formulation [4–8]. However, good levels of encapsulation efficiency are combined with the wastefulness of a large amount of active substance and the reduction of the cost-effectiveness of the process.

Microencapsulation is often proposed as a promising approach also to preserve the efficacy of plant aqueous extracts, to convert them from liquid to solid form, which is easier to handle, to improve the stability of their active compounds during processing and storage, and to guarantee a taste masking effect [9–11]. In some cases, when the goal is to microencapsulate polyphenols, which are the principal components of aqueous plant extracts, some authors suggest the immersion of dried placebo microparticles or beads directly into the aqueous extract for 24 h to permit the absorption of these compounds [12,13]. Nevertheless, this last approach is more challenging to keep under control, and the results obtained are often not so satisfying in terms of drug loading and reproducibility.

The *Thymus vulgaris* L. aqueous extract was selected as the active compound; it is renowned for its antioxidant, antimicrobial, and antifungal activity, but it requires protection to maintain these properties unchanged. The novelty of this work is associated with the strategy selected to improve the encapsulation efficiency represented by an effective formulation approach that first of all avoided the waste of the active compound and was reproducible and affordable.

The goal of this study was to increase the encapsulation efficiency of alginate-based microparticles containing thyme aqueous extract, by the use of several co-carrier excipients.

The microparticles were produced by ionic gelation. A starting formulation loaded with thyme extract and composed only of alginate as the structuring excipient has been selected as a reference and optimized with different co-carrier excipients able to perform various functions (fillers, strengthening of the polymeric network or forming an interpenetrating system) to limit the leakage of the highly soluble molecules. A complete characterization (encapsulation efficiency, process yield, dimensional and morphological analysis) was conducted on all batches of microparticles prepared. Moreover, a deeper investigation (SEM analysis, swelling study, release test, thermogravimetric analysis) was carried out on the most promising formulation among those containing alginate with other excipients and compared to the reference.

2. Materials and methods

2.1. Materials

Thymus vulgaris L. was provided by A. Minardi & Figli (Bagnacavallo, Italy). Low-viscosity sodium alginate (Protanal® LF 10/60) and medium-viscosity sodium alginate (Manucol® LKX 5) were gifted by Dupont Italia (Milan, Italy). High-viscosity sodium alginate and isolated soybean proteins 90 % were obtained by Farmalabor (Assago, Italy). Flaxseed flour (HI-SMOOTH) was purchased from HI–FOOD (Pilastro di Langhirano, Italy). Maltodextrin was provided by A.C.E.F. (Fiorenzuola D'Arda, Italy). Modified starch (CLEARGUM® CO 01) was purchased from Roquette (Lestrem, France). Carrageenan iota was obtained by CP Kelco (Lille Skensved, Denmark). Pectin (Pectin Amid *CF* 025-D) was procured by Herbstreith & Fox KG (Neuenbürg, Germany). Low molecular weight (LMW) – chitosan (degree of deacetylation >80 %) was kindly donated by Tidal Vision (Bellingham, USA), Shellac gum by SSB Stroever GmbH & CO. KG (Auf Der Muggenburg, Germany) and Diutan gum (KELCO-CARE™ Diutan Gum) by Biochim (Casarile, Italy). Hydroxyethylcellulose (NATROSOL® Pharm) was obtained by Ashland (Wilmington, USA).

All other reagents were of analytical grade and used as received.

2.2. Experimental methods

2.2.1. Preparation of thyme aqueous extract

The extract was prepared by weighing about 100 g of pulverized thyme leaves per 1 L of hydroalcoholic mixture (50 % *v*/v ethanol). The maceration was carried out under stirring for 2 h. After filtration with filter paper, the obtained extract was recovered and introduced into a rotating evaporator (Buchi, Rotavapor R-210, Flawil, Switzerland) equipped with a heating bath (B-491) and vacuum pump (V-100) to eliminate the alcoholic fraction. The water content of the resulting extract was determined by a thermobalance (Radwag, Ma 50/1.R.WH, Radom, Poland). The analysis was performed in triplicate.

2.2.1.1. Total phenolic content. The total phenolic content was determined using a modified version of the Folin–Ciocalteu method [14]. 50 μL of Folin-Ciocalteu reagent (Sigma-Aldrich, St. Louis, USA) and 175 μL of aqueous Na_2CO_3 (5 % *w*/v) were added to 50 μL of thyme aqueous extract, previously diluted (1:50). Then the solutions were made up to a final volume of 1450 μL with distilled water. After 1 h, the absorbance was determined at 760 nm using a UV spectrophotometer (Shimadzu-1900, Oregon, USA). Results were expressed as mg catechin equivalents per gram of dried extract.

2.2.1.2. HPLC analysis of phenolic compounds. The quantification of specific phenolic compounds present in the extract was performed using a Shimadzu LC-20 A Prominence chromatographic system (Oregon, USA) equipped with a diode array detector (DAD detector SPD-M20A). Separation was performed on a reversed-phase Phenomenex Luna C-18100 Å Column (150 × 2 mm, with a particle size of 5 μm) (Phenomenex, Torrance, CA, USA), protected by a guard column containing the same phase, at 30 °C. Eluent A was water/formic acid 0.1 % *v*/v, and Eluent B was acetonitrile/formic acid 0.1 % *v*/v (HPLC grade solvents). The elution program used (total run time: 80 min, flow rate: 0.4 mL/min) was set up as follows: from 5 % to 35 % B (40 min), from 35 % to 75 % B (13 min), from 75 % to 5 % B (7 min), isocratic 5 % B for equilibration of the column (20 min). The volume injection was 5 μL. Chromatograms were recorded at 280 nm and 330 nm, and the scan was performed between 200 and 260 nm. Specific phenolic compounds were determined by comparing the retention times and spectral data of standards, while the quantification was carried out using a calibration curve of each standard. Analyses were replicated three times, and the results were expressed as μg of specific compound/g of dried thyme extract.

2.2.2. Encapsulation of thyme extract by ionotropic gelation

2.2.2.1. Preliminary phase. In a preliminary phase, three basic formulations, made of thyme aqueous extract and low-viscosity alginate, were prepared to be processed by ionotropic gelation. They differed from each other for the final ratio between thyme extract and alginate in the dried microparticles: 70:30 (TA1), 50:50 (TA2), and 30:70 (TA3). All the starting solutions had the same alginate concentration (2.5 % *w*/w). For the TA1 formulation, sodium alginate was solubilized directly into the aqueous extract, while in the case of TA2 and TA3 formulations, a previous dilution of the extract was required before the addition of alginate to achieve the desired ratio between extract and polymer.

Each formulation (about 20 g) was dripped into a gelling bath (500 mL calcium chloride aqueous solution 100 mM) with a syringe (21G needle = 0.80 mm internal diameter) placed 10 cm away from it. The

newly formed beads were maintained under curing for 15 min, then they were recovered by filtration, washed with deionized water, and dried for 1 h by dynamic drying in a fluid bed dryer under airflow at 27 °C.

2.2.2.2. Optimization phase. Optimization of the most promising basic formulation with the addition of co-carrier excipients was set up to improve the encapsulation efficiency. In some cases, the gelling bath concentration or the solvent of the gelling bath was modified, as reported in Table 1. The co-carrier excipients were added directly to the basic formulation as such. Chitosan was the only one that was not included in the formulation to be dripped, but it was added to the gelling bath at the concentration indicated in Table 1. The difference between F9 and F10 formulations was the pH of the gelling bath: in the first case, it was 4.52, while for F10, it was 3.29. Shellac gum was used as a 5 % *w*/w solution, which was prepared according to the method described by Foglio Bonda *et al.* [15]: shellac gum was solubilized in 0.5 % *w*/w ammonium carbonate solution at 50 °C; the obtained solution was heated to 60 °C until a constant pH, indicative of the complete elimination of the ammonium salt excess, was reached. After replacing the evaporated water, the shellac gum solution was diluted with alginate/thyme solution until the required concentration was obtained.

All formulations were submitted to ionotropic gelation according to the procedure described above and characterized regarding morphology, dimensions and encapsulation efficiency. Only the technological properties of the most satisfying system were deeply investigated.

2.2.3. Characterization of the microparticles

2.2.3.1. Encapsulation efficiency and process yield. The encapsulation efficiency (EE) was calculated as the weight of thyme extract loaded into microparticles divided by the theoretical one, according to Eq. (1). The thyme extract loaded into microparticles was obtained by subtracting the amount of thyme extract present in the gelling bath after the microparticle curing time from the theoretical one. The concentration of thyme extract in the gelling bath was determined spectrophotometrically at 282 nm.

$$\text{EE}\ (\%) = \frac{\textit{Weight of the actual loaded thyme extract}}{\textit{Weight of the theoretical loaded thyme extract}} \times 100 \quad (1)$$

The process yield (PY) was calculated using Eq. (2). The "weight of actual solids" was the weight of the obtained dried microparticles, and the "weight of theoretical solids" was the sum of the weight of alginate powder and thyme extract in the case of basic formulations. At the same time, it was the sum of alginate, thyme extract, and co-carrier excipient used for the optimized formulations.

$$\text{PY}\ (\%) = \frac{\textit{Weight of actual solids}}{\textit{Weight of theoretical solids}} \times 100 \quad (2)$$

Table 1
Formulations tested in the optimization phase.

	Carrier excipients	Excipient conc. (% w/w)	Gelling bath [$CaCl_2$] (M)	Gelling bath solvent
F1	High viscosity alginate	0.50	0.1	Water
F2	Medium viscosity alginate	0.50	0.1	Water
F3	Soybean protein	0.50	0.1	Water
F4	Flaxseed flour and maltodextrin	1.00	0.1	Water
F5	Modified starch	0.50	0.1	Water
F6	Carrageenan iota	0.50	0.1	Water
F7	Pectin	0.50	0.1	Water
F8	Pectin	2.00	0.5	Water
F9	Chitosan	0.20	0.1	Acetic acid 0.1 %
F10	Chitosan	0.20	0.1	Acetic acid 1.0 %
F11	Chitosan	0.50	0.1	Acetic acid 1.0 %
F12	Shellac gum	0.50	0.1	Water
F13	Diutan gum	0.05	0.1	Water
F14	Hydroxyethylcellulose	0.50	0.1	Water

2.2.3.2. Morphological and particle size analysis. All batches of microparticles were inspected by optical microscopy (Stereomicroscope Leica-S9i, Wetzlar, Germany). Each sample was photographed immediately after the preparation (in the swollen state, wet microparticles) and after the drying process (dried microparticles). The average diameter (Z_D) and shape factor (SF) of wet and dried microparticles (at least 20 units) were determined using image analysis software Image J 1.501 (National Institute of Health, Bethesda, MD, USA) [16]. All the results were submitted for statistical analysis using a one-way analysis of variance (ANOVA) and *post hoc* Tukey test. The statistical significance level was set at 0.05.

The polydispersity index (PDI), associated with the size distribution of the microparticles, was calculated using Eq. (3) [17], where Z_D represents the average diameter of the beads and σ the standard deviation of Z_D.

$$\text{PDI} = \frac{\sigma^2}{{Z_D}^2} \quad (3)$$

The distribution was considered monodispersed for PDI ≤ 0.1 and polydispersed for higher PDI values. Moreover, for each batch of microparticles, the percentage of dimensional decrease (DD) between wet and dried systems and the percentage of dimensional increase (DI) among TA3 and F10 (in the wet and dried state) were calculated according to the Eq. (4), where Z_D is the average diameter of the microparticles.

$$\text{Dimensional variation}\% = 100 - \left(\frac{Z_D\ lower}{Z_D\ higher} \times 100\right) \quad (4)$$

In addition, TA3 and F10 microparticles were submitted to a more detailed investigation of their structure and morphology using scanning electron microscopy (SEM) (Phenom XL, Thermo-Fischer Scientific, Waltham, MA, USA) at 15 kV voltage after the gold coating of the particle's external surface.

2.2.3.3. Swelling properties. The swelling of TA3 and F10 dried microparticles in water, phosphate buffer (PBS) 0.1 M (pH 6.8), and HCl pH 1.0 was evaluated to determine their behavior after contact with fluids characterized by different pH values. An amount of each sample (about 10 beads) was weighed and introduced in a vial in which 5 mL of the selected fluid was added. Every vial was maintained at room temperature, and after predefined time intervals (15, 30, 60, and 120 min), the microparticles were recovered and weighed again. The swelling percentage was calculated using Eq. (5), where W_t represents the sample weight after contact with each fluid, and W_0 is its initial weight [18].

$$\text{SW}\% = \frac{W_t - W_0}{W_0} \times 100 \quad (5)$$

The data were expressed as the mean of three determinations ± standard deviation. Statistical analysis was carried out by one-way analysis of variance (ANOVA), followed by the *post hoc* Tukey test, to investigate the differences between groups. The statistical significance level was set at 0.05.

2.2.3.4. Flowability. The flowability of TA3 and F10 dried microparticles was evaluated by the determination of the dynamic angle of repose using a hollow transparent cylinder (diameter: 3.0 cm; height: 1.5 cm) linked to an overhead stirrer [19]. The cylinder was filled with an adequate amount of microparticles (about 100 mg) to create a measurable angle of repose. During the test, some photos were taken and

then analyzed with Image J software to calculate the angle of repose. When keeping the stirrer speed constant, the maximum angle formed by the oblique plane with the horizontal one during the rotation of the cylinder was assumed as the angle of repose. The data were reported as the average of three determinations for each sample. The flowability was defined according to the European Pharmacopeia classification [20].

2.2.3.5. Thermogravimetric analysis. The thermal behavior of thyme extract, TA3, and F10 microparticles and the corresponding systems without thyme extract (placebo), the single polymeric carrier (alginate and chitosan) was investigated by thermogravimetric analysis (TGA) using the Thermogravimetric Analyzer (TGA 4000 model, Perkin Elmer, Milan, Italy). An exactly weighed amount of each sample was heated in a standard ceramic sample pan. The analyses were carried out in the 25 to 600 °C temperature range at a 10 °C/min scan rate under nitrogen purge (20 mL/min).

2.2.3.6. Thyme extract content and release test. The experimental thyme extract content of dried microparticles was determined after complete disaggregation and dissolution of the systems in PBS 0.1 M (pH 6.8). In detail, exactly weighed amounts of TA3 and F10 microparticles (about 25 mg) were put in 25 and 30 mL of PBS at pH 6.8, respectively, and maintained under stirring until complete dissolution. The obtained solution was analyzed by UV–Vis spectrophotometer (Beckman Coulter DU® 730, Brea, USA) at 282 nm wavelength to determine the thyme extract concentration and calculate the percentage of thyme extract loaded in microparticles referring to the experimental calibration curve ($R^2 = 0.998$, Eq. (6)).

$$y = 0.008x + 0.0149 \quad (6)$$

The data are obtained as the relation between the analyte concentration of the samples tested (30, 40, 60 and 80 μg/mL) and their UV absorbance. The results are the average of three determinations.

TA3 and F10 dried microparticles were submitted to release tests to assess the amount of thyme extract released in PBS 0.1 M (pH 6.8) over time. For each type of microparticle, about 25 mg were exactly weighed, put in a precise volume of fluid (25 mL for TA3; 30 mL for F10), and kept under stirring (300 rpm) at 37 °C. At different time intervals (15, 30, 45, and 60 min), an aliquot of solution (3 mL) was withdrawn with replacement, filtered by 0.22 μm filter, and analyzed spectrophotometrically at 282 nm wavelength. The percentage of thyme extract released after each interval was calculated considering the experimental thyme extract content of each system. TA3 and F10 release profiles were statistically compared using the dissolution similarity factor (f2): the curves were considered similar with f2 values > 50 [21].

2.2.3.7. Release kinetic study. As presented below, several mathematical models were applied to understand the thyme release kinetics.

Higuchi:

$$F(t) = k \times t^{0.5} \quad (7)$$

$$F(t) = 100 \times \left(1 - C \times exp^{(-k \times t)}\right) \quad (8)$$

where F(t) represents the amount of the compound released at time t and k is the release constant. Eq. (7) is Eq. (2.12) from [22].

Peppas-Sahlin:

$$F(t) = k_1 \times t^m + k_2 \times t^{(2 \times m)} \quad (9)$$

where F(t) represents the amount of the compound released at time t, k_1 is the diffusion constant, k_2 is the erosion constant and m is the diffusional exponent, representing the release mechanism.

Ritger-Peppas:

$$F(t) = k \times t^n \quad (10)$$

where F(t) represents the amount of the compound released at time t, k is the release constant and n is the release exponent, representing the release mechanism.

Zero-order:

$$F(t) = k \times t \quad (11)$$

where F(t) represents the amount of the compound released at time t and k is the release constant.

Korsmeyer-Peppas:

$$F(t) = k_{KP} \times t^n \times Q_0 \quad (12)$$

where F(t) represents the amount of the compound released at time t, k_{KP} is the release constant, n is the release exponent, representing the release mechanism, and Q_0 corresponds to the initial amount of the compound.

3. Results and discussion

3.1. Thyme aqueous extract characteristics

The obtained thyme aqueous extract, characterized by 93.27 ± 0.05 % of water content, was submitted to the determination of total phenolic compounds. The experimental analysis resulted in 172.66 ± 6.72 mg of catechin equivalent per g of dried extract. In addition, each phenolic compound included in the thyme extract was quantified by HPLC analysis (Table 2), and in agreement with the literature, rosmarinic acid was the phenolic compound present in the highest quantity [23].

3.2. Preliminary phase

The use of ionotropic gelation to microencapsulate a highly soluble compound represents an interesting research challenge, as reported in the literature [24,25], because its rapid diffusion out of the newly formed microparticles into the gelling bath is responsible for a not always satisfying encapsulation efficiency.

Three alginate microparticle batches were prepared by ionotropic gelation starting from three aqueous solutions composed of alginate as carrier excipient and thyme extract at different loading. All three formulations were demonstrated to be suitable for obtaining cross-linked alginate microparticles even if with a dissimilar process yield (PY) that decreases according to the following order TA3 > TA2 > TA1, and it was respectively 74 %, 62 %, and 44 %. These results may be strictly correlated to microparticle composition: a high percentage of alginate in the formulation corresponds to a more resistant polymeric cross-linked network that forms after microparticle curing in the gelling bath. This represents an important aspect to be considered to guarantee the obtainment of microparticles with adequate mechanical resistance and to avoid or limit the loss of material because of a structural collapse.

Regarding the appearance of the microparticles, TA1 samples,

Table 2
Phenolic compounds included in the thyme aqueous extract.

Phenolic compound	μg/g of dried extract
Rosmarinic acid	23,914.0 ± 805.0
Vanillic acid	85.5 ± 5.2
Syringic acid	618.2 ± 23.2
Chlorogenic acid	499.6 ± 8.6
Caffeic acid	2160.9 ± 126.9
Ferulic acid	1115.4 ± 49.1
Ellagic acid	1270.6 ± 65.1
Quercetin	880.1 ± 18.1
Luteolin	2526.8 ± 97.1
Apigenin	198.1 ± 13.2
Kaempferol	175.7 ± 6.6
Epicatechin	1487.1 ± 53.4
Rutin	346.1 ± 16.6

mainly the wet ones, showed the worst shape (shape factor values below 0.85, Table 3) and were characterized by some surface irregularities (Fig. 1).

The SF of dried microparticles slightly decreased compared to the SF of wet systems as a consequence of the polymeric network shrinkage due to water evaporation and the formation of biconcave disk shape microparticles associated with a flattening and partial collapse of the calcium-alginate network. The results of the particle size analysis showed that all the samples were monodispersed in size, as confirmed by the PDI value being lower than 0.1. Immediately after the preparation, all microparticles were quite large in dimensions, and their average diameter exceeded abundantly 2 mm: it was between 2.4 and 2.8 mm. At the dried state, the highest concentration of alginate (about 70 % *w*/w) in the formulation (TA3) was responsible for the obtainment of microparticles larger in diameter compared to TA1 and TA2.

The EE (%) values of the three basic formulations were too low and not acceptable: the thyme extract encapsulated is always halved compared to the initial one because it tended to diffuse out of the microparticles into the gelling bath, driven by the concentration gradient. In detail, EE was 55.29 ± 0.09 %, 47.11 ± 0.46 %, and 56.87 ± 0.52 % for TA1, TA2, and TA3, respectively.

Given the unsatisfying EE results, it was necessary to improve this aspect by modifying the starting formulation: TA3 was selected and used as a reference mainly for its PY and appearance/morphology results.

3.3. Formulation study

The selected starting formulation (TA3) was enriched with co-carrier excipients that were able to retain the hydrophilic thyme extract better in the microspheres. The literature suggests several strategies to overcome this limit like the use of a mixture of alginates with different viscosities, the variation of calcium-chloride concentration in the gelling bath, the saturation of the gelling bath with the encapsulated active compound, or the addition of fillers to the solution/dispersion to be processed to improve the total solid amounts [5,6,26]. Different formulation tests were performed, and different types of co-carrier excipients were selected to have components capable of performing various functions, aiming to identify the most suitable one. High and medium molecular weight sodium alginates were selected as strengthening carriers; soybean protein, flaxseed flour, maltodextrin, and modified starch as fillers to give the microparticles a more solid structure; carrageenan iota, pectin, LMW chitosan, shellac gum, diutan gum, and hydroxyethylcellulose (HEC) as polymers able to form interpenetrating systems [27,28].

In general, the process yields of the ionic gelation carried out on the improved formulations increased compared to that of TA3 and were included between 75 and 95 %. This result could be attributed to the presence of an extra component in the formulation responsible for the increase of the initial concentration of solids and its ability to support the structure of the microparticles.

Regarding the EE, it varied between 40 % and 70 %. In many cases (F2, F5, F6, F7, F8, F9, F11 e F13), the EE was similar to that obtained with TA3 formulation, without gaining any improvement. In general, the EE obtained with the additional excipients did not overcome 62 %, demonstrating that the inclusion of a co-carrier is only sometimes a valuable strategy to improve the entrapment of the active substance. In some cases (F1, F3, F4, and F12), the tested excipients led to a worsening of EE compared to the reference formulation because they may have increased the distance between the polymeric chains, making the porosity of the microparticle and the loss of the aqueous extract higher. One of the lowest EE is associated with the formulation containing sodium alginate at high viscosity (F1). The reason for this unsatisfying result could be found in the monomer composition and arrangement of the selected polymer because alginate's structure-forming and gelation properties are highly dependent on them. As reported in the literature, gel formation and cross-linking reactions are due to the interactions between guluronic residues and divalent cations [29]. The alginate at high viscosity grade used in this work had an M/G ratio indicative of the predominance of mannuronic residues in its polymeric chains, which are not those responsible for forming strong and resistant gels. Probably, the egg-box structure formed was characterized by quite large network meshes that the hydrophilic extract could use to move towards the gelling bath, reducing its content into the microparticles. Only the F10 formulation gave ameliorated EE (about 70 %) compared to that of TA3.

Stereomicroscope images of wet and dried microparticles of each formulation were compared (Fig. 2). Overall, the wet microspheres (except F3 and F4) had a smooth, homogenous, and regular surface and a quite spherical shape as attested by SF close to 1 (Table 4). F3 wet microparticles were not uniform in color because of the poor dispersion of the soybean protein (insoluble) and then of the encapsulated extract. F4 particles showed an irregular shape because the high viscosity of the formulation made its extrusion through the needle difficult and caused the formation of more elongated droplets and, consequently, not-so-rounded particles.

After drying, regardless of the formulation composition, the size of microparticles was widely reduced, as indicated by the dimensional decrease values (DD in Table 4), because of the water evaporation, the microparticle shrinkage, and the packing of polymeric chains. As visible in the stereomicroscope images (Fig. 2, B lines), the drying process was overall also responsible for a worsening of the shape of microparticles, which became irregular and moved away from sphericity as demonstrated by the SF values far from 1 (Table 4).

All the samples had higher diameters compared to TA3 due to an increment of dry matter content and/or of the viscosity of the starting material that, consequently, led to larger droplets and larger microparticles (Table 4). Wet microparticles had a mean diameter between 2.5 and 3.5 mm, while in the case of the dried systems, these values were between 0.9 and 1.5 mm, and all the batches were monodispersed as regards particle size distribution. The dimensions of microparticles produced using the improved formulations were dependent on the characteristics of the excipient selected as a co-carrier and were not related to the EE results. In general, the decrease in microparticle diameter should be responsible for an increase in its surface area; this should accelerate the diffusion of the active substance out of the polymeric network, which is responsible for an unsatisfying encapsulation efficiency. On the contrary, high diameters and low surface area should drive towards good levels of EE. In this work, even if the lowest EE was recorded for the microparticles characterized by the smallest particle size, the highest EE was not associated with the biggest one. F9 microparticles (both wet and dried) showed not only the highest dimensions but also the most irregular shape, above all at the dried state: their SF did not exceed 0.75, and this is indicative of elliptical and elongated shapes. F9 were alginate-chitosan microparticles prepared according to the single-step method reported in the literature [30,31], in which the gelling bath is characterized by diluted acetic acid (0.1 %) as solvent; the obtained results about their aspect, morphology, and EE were an unexpected outcome compared to the results reported by other authors

Table 3
Dimensional and morphological analysis of TA1, TA2, and TA3. $\mathbf{Z_{Dw}}$ is the mean diameter of wet microparticles while $\mathbf{Z_{Dd}}$ is the one of dried microparticles; **DD** is dimensional decrease; **PDI** is the polydispersity index, and **SF** is the shape factor. Different letters indicate significant differences among the mean diameters ($p < 0.05$).

	TA1	TA2	TA3
Z_{Dw} (μm) ± sd	2453.10 ± 193.56[a]	2779.22 ± 131.89[b]	2644.42 ± 126.50[b]
Z_{Dd} (μm) ± sd	856.69 ± 50.97[a]	923.55 ± 48.86[b]	1015.48 ± 39.95[c]
DD (%)	65.08	66.77	61.60
PDI wet	0.00623	0.00225	0.00229
PDI dried	0.00354	0.00280	0.00155
SF – wet ± sd	0.82 ± 0.08	0.88 ± 0.06	0.92 ± 0.04
SF – dried ± sd	0.84 ± 0.07	0.84 ± 0.09	0.83 ± 0.08

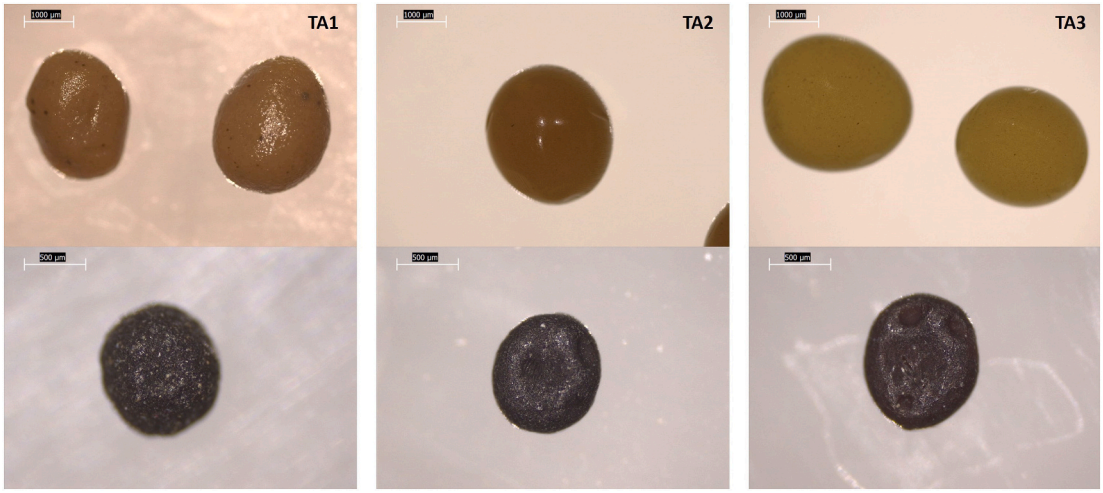

Fig. 1. Stereomicroscope images of TA1, TA2, and TA3 microparticles immediately after the preparation (above, magnification 20×) and after the drying process (below) (magnification 50×).

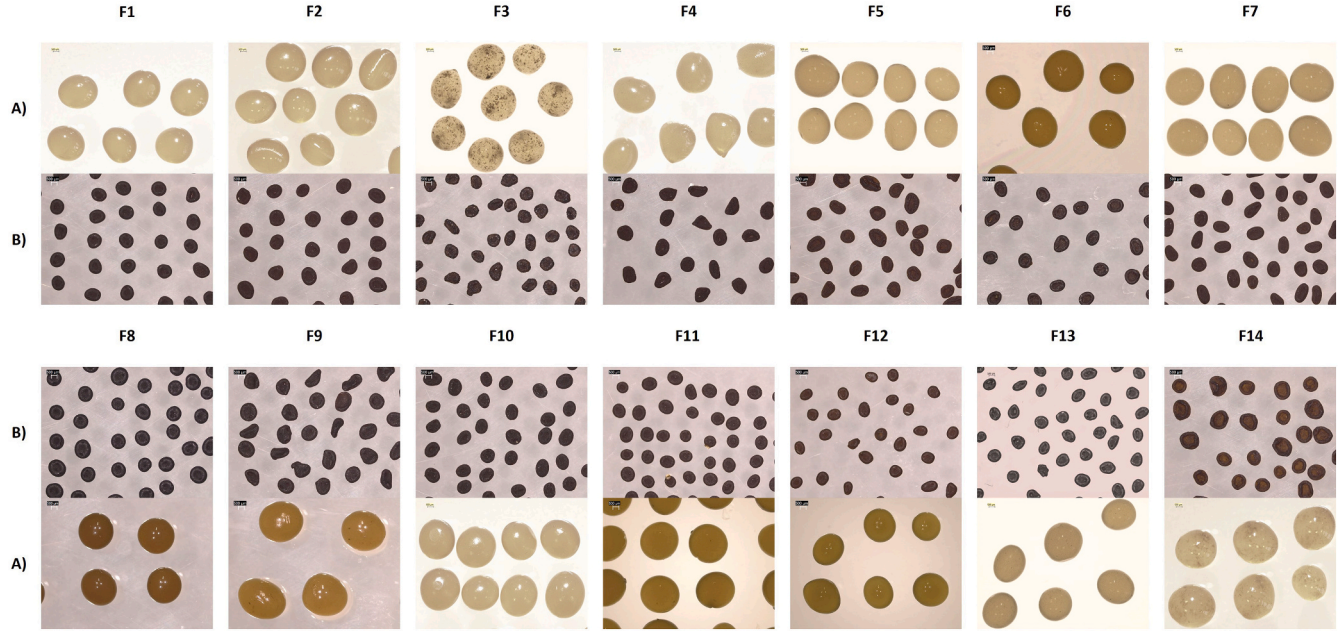

Fig. 2. Stereomicroscope images of wet (A) and dried (B) microparticles obtained from improved formulations (magnification10×).

Table 4
Dimensional and morphological properties of microparticles obtained in the formulation study.

	Z_{Dw} (μm) ± sd	Z_{Dd} (μm) ± sd	DD (%)	PDI wet	PDI dried	SF – wet ± sd	SF – dried ± sd
F1	2952 ± 95	1276 ± 35	56.76	0.001	0.001	0.90 ± 0.04	0.84 ± 0.07
F2	3160 ± 242	1270 ± 73	59.79	0.006	0.003	0.91 ± 0.07	0.86 ± 0.07
F3	2903 ± 129	1146 ± 73	60.51	0.002	0.004	0.90 ± 0.06	0.81 ± 0.11
F4	3242 ± 105	1273 ± 60	60.73	0.001	0.002	0.86 ± 0.07	0.76 ± 0.11
F5	3035 ± 295	1316 ± 124	56.62	0.009	0.009	0.87 ± 0.06	0.77 ± 0.09
F6	3064 ± 159	1224 ± 60	60.05	0.003	0.002	0.90 ± 0.05	0.83 ± 0.07
F7	3307 ± 185	1222 ± 70	63.06	0.003	0.003	0.86 ± 0.04	0.73 ± 0.10
F8	2931 ± 60	1306 ± 120	55.45	0.001	0.008	0.95 ± 0.03	0.93 ± 0.04
F9	3466 ± 103	1480 ± 92	57.31	0.001	0.004	0.86 ± 0.06	0.74 ± 0.13
F10	2981 ± 211	1096 ± 72	63.22	0.005	0.004	0.92 ± 0.04	0.88 ± 0.06
F11	3009 ± 173	1108 ± 98	63.17	0.003	0.008	0.91 ± 0.04	0.88 ± 0.06
F12	2508 ± 204	931 ± 72	60.42	0.007	0.005	0.91 ± 0.04	0.82 ± 0.09
F13	2812 ± 155	897 ± 74	68.11	0.003	0.007	0.87 ± 0.07	0.81 ± 0.10
F14	3345 ± 355	1442 ± 166	56.89	0.011	0.013	0.92 ± 0.03	0.89 ± 0.04

[28–30]. However, the application of this production protocol was not so satisfying because when the alginate solution drops fell into the $CaCl_2$ bath to which chitosan was added, alginate was rapidly cross-linked causing the formation of a polymeric porous structure embedding more water and, at the same time, leaking the aqueous extract.

Some authors used chitosan as a co-carrier not to improve the encapsulation efficiency but to modify and decrease the drug release rate; they proposed a method in which the dripping of the formulation was carried out into an acid-gelling bath [32,33]. To evaluate if this strategy could also be more incisive in the improvement of EE, it was applied to the production of F10 microparticles. The resulting EE (70.43 ± 5.28 %) confirmed the correctness of the choice. The availability of more H^+ ions in the gelling bath, compared to that used for producing F9 microparticles, reduced the proportion of ionized carboxylic groups in the alginate structure and, consequently, its solubility as well as the network porosity. Moreover, the aminic sites of chitosan were positively charged, becoming able to react with the remaining groups -COOH of the alginate, creating a more impermeable shell around the droplet which retained the thyme extract [34].

The increase of chitosan concentration in the bath (F11) was not responsible for a significant variation in particle size (F10 and F11 microparticles had similar dimensions both in the wet and dried state) and shape. Moreover, it also did not have a positive effect on the encapsulation efficiency, and this behavior is in line with those reported by Motwani *et al.* and Takka and Gùrel [35,36].

According to the results, the F10 formulation was selected as the best one, and F10 microparticles were completely characterized and compared to the reference (TA3).

The experimental thyme extract content of TA3 and F10 dried microparticles was 17.606 ± 0.158 % and 20.087 ± 1.487 % respectively.

Both samples were observed using an optical stereomicroscope and SEM (Fig. 3–4): it can be noticed that F10 microparticles (composed of alginate and chitosan) were larger in diameter than TA3, as reported also by Boskov *et al.* [37]. The particle size increase, corresponding to 11.28 % in the wet state and 7.37 % in the dried state, was attributable to the presence of a polyelectrolytic blend in the microparticle structure resulting from the electrostatic bindings between chitosan and alginate, furtherly promoted by the acidic environment of the gelling bath. The production protocol adopted, which involves the inclusion of the second carrier excipient (chitosan) in the gelling bath, allowed the deposition and/or interaction of this polymer on the surface of the drops of alginate solution just when they come in contact with the gelling bath. The presence of calcium ions and chitosan in the bath at the same time modified the dimensions of the final product and probably also the structure of its network structure [30]. Observing the cross-section of the F10 microparticles in the stereomicroscope images (Fig. 3), it was possible to identify an external layer, which may be due to the interpenetration of chitosan into the most external layer of the alginate egg-box network. SEM images (Fig. 4) confirmed that the two batches of microparticles were not identical. The internal surface of TA3 and F10 microparticles was similar and appeared dense, smooth, and homogeneous, but some relevant differences were visible in correspondence of the external layer. F10 microparticles had a more wrinkled and organized external surface than TA3 (Fig. 4) due to the strong polyelectrolytic interaction between alginate and chitosan [38]. In both cases, pores, fractures, or ruptures were not visible, indicating the structural integrity of the systems.

3.4. Flowability

The surface irregularities highlighted by the morphological analysis negatively influenced the flowability properties of both batches of microparticles. The angle of repose of TA3 was 49.67 ± 3.06°, while that of F10 was 43.33 ± 2.08°, leading to poor and passable flowability, respectively. The aptitude to flow of F10 microparticles was slightly better thanks to their more rounded shape, as confirmed by the SF value, and this represents an added value that can simplify their processing and handling.

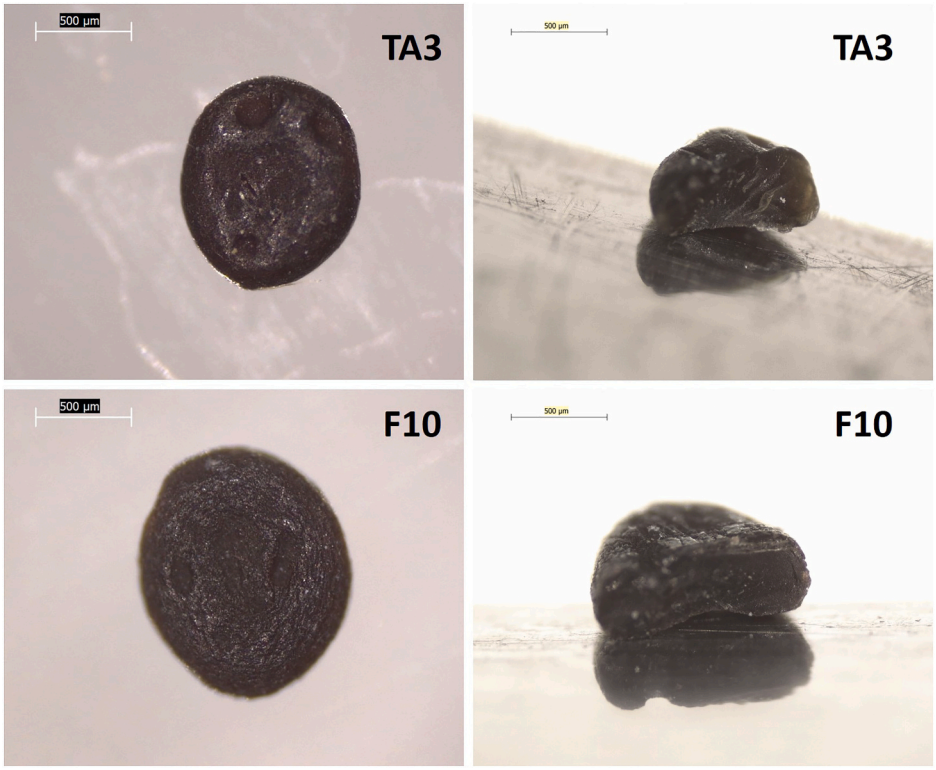

Fig. 3. Stereomicroscope images of the external surface and cross-section of TA3 and F10 dried microparticles (magnification 10×).

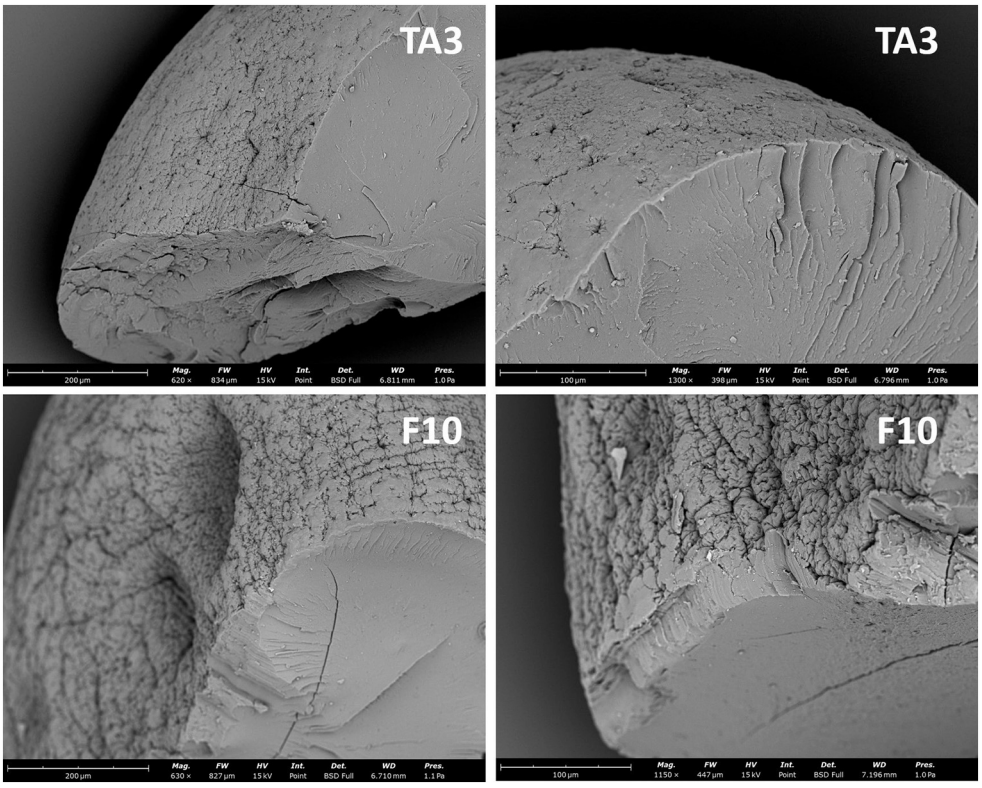

Fig. 4. SEM images of the external surface and cross-section of TA3 and F10 dried microparticles (620× and 1300× magnification for TA3 and 630× and 1150× magnification for F10).

3.5. Thermogravimetric analysis

The thermogravimetric behavior of TA3 and F10 microparticles in the absence (placebo) and with the thyme extract is reported in Figs. 5 and 6, respectively, compared to that of the single polymers (alginate and chitosan).

The weight losses occurring above 180 °C in all the profiles were ascribable to the dehydration of the alginate and chitosan polymeric matrix [39,40]. The free and bound water content percentages for alginate and chitosan were about 17 % and 10 %, respectively. At temperature above 180 °C, the curve of alginate presented other degradation events due to the breaking of glycosidic bonds, decarboxylation, and decarbonylation of the polymeric structure [39], while the thermal step in the profile of chitosan between 200 and 500 °C was mainly attributed to the decomposition of the saccharide rings [40].

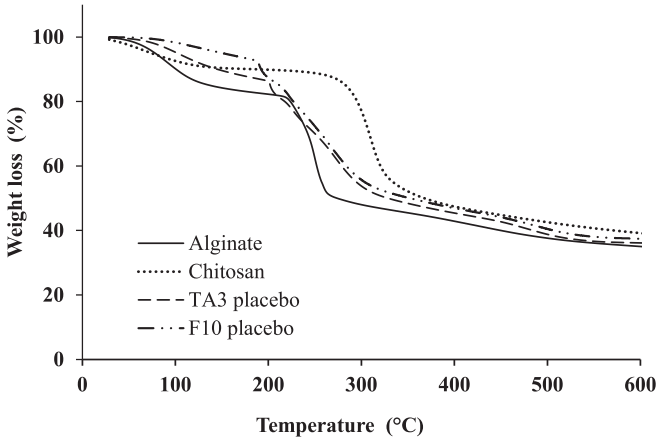

Fig. 5. Thermogravimetric profiles of alginate, chitosan, TA3 placebo and F10 placebo microparticles.

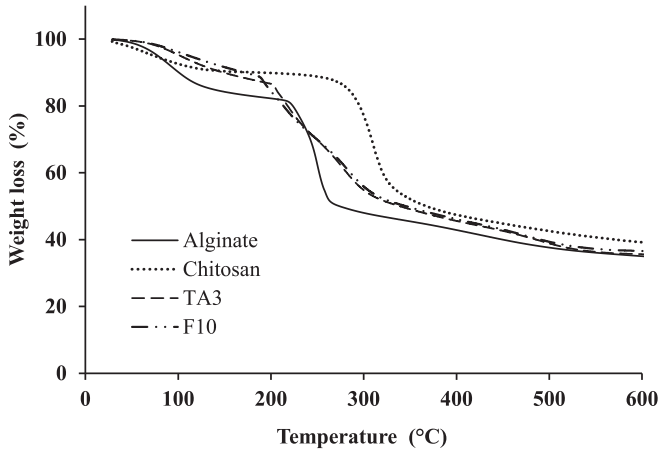

Fig. 6. Thermogravimetric profiles of alginate, chitosan, TA3 and F10 microparticles.

The TGA profiles of the microparticles appeared as the results of the single components. However, comparing the first step of the curves, it can be observed that microparticles containing chitosan (F10) were characterized by lower water content percentages: 6.9 % for F10 placebo and 10.5 % for F10 *vs* 12.4 % and 12.1 % for TA3 placebo and TA3, respectively. These results suggested that chitosan, both in the presence or absence of thyme extract, was able to improve the drying of alginate microparticles.

As expected, the presence of thyme extract in the microparticles TA3 and F10 did not influence the degradation behavior of the excipients nor the role of chitosan in reducing the water content in drying the polymeric systems.

3.6. Swelling properties

The swelling behavior of TA3 and F10 dried microparticles was evaluated in deionized water, PBS pH 6.8, and HCl pH 1.0. As illustrated in Figs. 7–8, the collected results of both samples in HCl and water were quite similar, demonstrating that the presence of chitosan did not significantly modify the swelling ability of the reference systems composed only of calcium-alginate (TA3 microparticles). In detail, the maximum swelling percentage in water was about 41 % for TA3, and it was slightly lower for F10 (about 35 %), probably because the presence of chitosan increased the entangled density of the systems due to the polyelectrolytic complex between the hydrophilic groups of the calcium-alginate network and the amino groups of chitosan which made the entry of fluid difficult. In a low-pH environment (HCl fluid), the swelling ability of microparticles was constant over time and not particularly pronounced, and although there was a difference in composition between TA3 and F10, the swelling results were comparable. After 15 min, microparticles increased their weight, reaching approximately 40 % of the swelling percentage; this value did not change significantly during the whole test. In PBS, the gap between the swelling behavior of microparticles became wide, mainly after 2 h. In this fluid, TA3 microparticles, characterized by an alginate polymeric network, swelled thanks to the Ca^{2+} and Na^{+} exchange, deriving from the calcium-alginate network and sodium phosphate salts. Instead, the swelling of F10 microparticles, in which alginate and chitosan were the polymeric carriers, was also due to the weakening of the alginate-chitosan interactions because the increase of pH lowered the number of cationic amino groups of chitosan [30]. In both cases, the highest swelling ratio in PBS was followed by the progressive disintegration of the beads.

3.7. Release study

The release profiles of thyme from TA3 and F10 systems in PBS pH 6.8 are shown in Fig. 9. After 15 min from the beginning of the test, >20 % of the extract in the case of TA3 and >34 % for F10 were in solution, and the release process ended in about 1 h. Even if, according to the starting phases of the release, it seemed that TA3 and F10 systems were not similar in their behavior, differently from the expectation, the influence of chitosan (F10) was not significant on the totality of the release process. TA3 and F10 release curves were similar as demonstrated by the similarity factor value (f2 = 53.31). The reason for the initial dissimilarity could be due to the difference between the composition of F10 and TA3 microparticles. Indeed, the chitosan in the F10 polymeric network slightly increased the swelling ability of the systems, as reported in the literature [38] and confirmed in this work by the swelling test results in PBS, making the fluid uptake easier and faster. Moreover, being diffusion and polymer swelling/relaxation the driving force of the release, the highest thyme extract content in F10 microparticles compared to TA3 ones increased the concentration gradient and promoted the outcome of the extract in the early phases of the process.

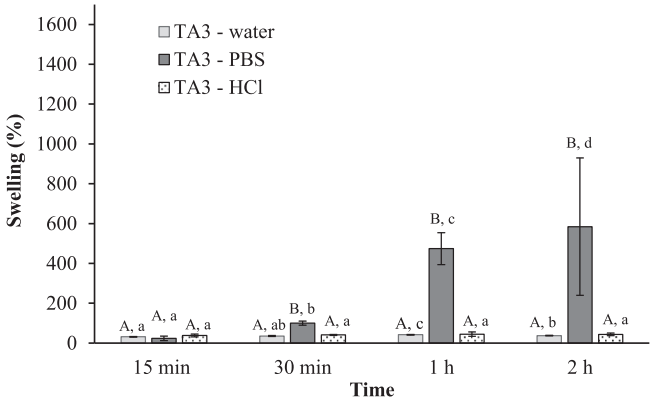

Fig. 7. Swelling behavior of TA3 microparticles in water, PBS, and HCl. Different uppercase letters indicate significant differences among the fluids at the same time intervals ($p < 0.05$). In contrast, distinct lowercase letters demonstrate significant differences between the time intervals of the sample in the same fluid ($p < 0.05$).

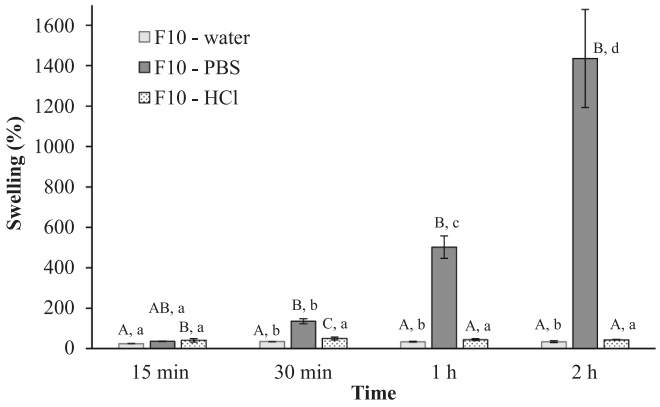

Fig. 8. Swelling behavior of F10 microparticles in water, PBS, and HCl. Different uppercase letters indicate significant differences among the fluids at the same time intervals ($p < 0.05$), while distinct lowercase letters demonstrate significant differences between the time intervals of the sample in the same fluid ($p < 0.05$).

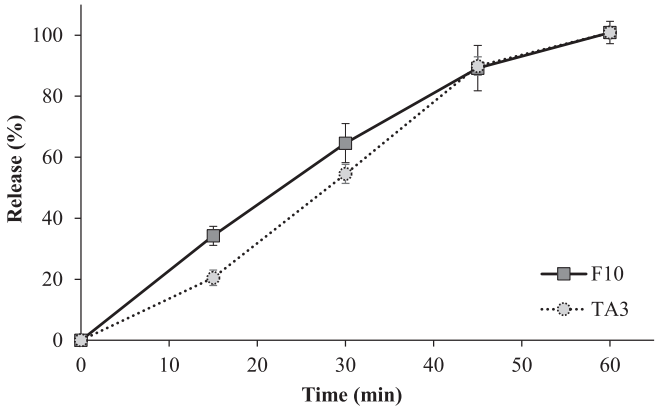

Fig. 9. Thyme extract release profiles of F10 and TA3 microparticles.

3.8. Release kinetic study

The mechanism of the thyme release from alginate (TA3) and alginate-chitosan (F10) microparticles is the combination of diffusional and relaxational contributions, associated respectively with the diffusion of the extract out of the systems and the swelling/erosion of the polymeric network. This assumption is demonstrated by the results reported in Table 5. The experimental data fit Ritger–Peppas and Korsmeyer–Peppas models with an $\mathbf{R^2}$ >0.97, and they fit better Peppas-Sahlin equation with an $\mathbf{R^2}$ = 0.9846 and $\mathbf{R^2}$ = 0.9902 for alginate-chitosan and alginate systems respectively. In both cases, k_1 was greater than k_2, indicating that the release was mainly controlled by Fickian diffusion.

4. Conclusion

The addition of chitosan to alginate-based microparticles turned out to be a promising strategy to encapsulate high percentages of an aqueous extract successfully. In particular, the suitable ratio between alginate and thyme aqueous extract and, mainly, the use of proper concentration

Table 5
Results of release model fitting. Kinetic elaborations were performed on release data obtained from at least three independent experiments for each batch.

Model	Equation	Form.	Coefficients (95 % confidence bounds)	Sum of squares	R^2	Degrees of freedom
Higuchi	$F(t) = k \times t^{0.5}$	TA3	k = 521.6 (457.3, 586.0)	5,668,253	0.8728	14
		F10	k = 652 (603.4, 700.5)	3,227,832	0.9439	14
Higuchi (Eq. 2.12 from [22])	$F(t) = 100 \times \left(1 - C \times exp^{(-k \times t)}\right)$	TA3	k = −0.03073 (−0.04051, −0.02261)	6,054,767	0.8642	13
		F10	k = −0.02683 (−0.03572, −0.01930)	8,981,767	0.8439	13
Peppas-Sahlin	$F(t) = k_1 \times t^m + k_2 \times t^{(2 \times m)}$	TA3	k_1 = ~ −24,435 k_2 = ~ 20,627 m = ~ 0.07323	438,493	0.9902	12
		F10	k_1 = ~ −15,885 k_2 = ~ 13,445 m = ~ 0.09198	888,727	0.9846	12
Ritger-Peppas	$F(t) = k \times t^n$	TA3	k = 82.68 (42.18, 151.6) n = 0.9889 (0.8317, 1.161)	1,105,283	0.9752	13
		F10	k = 248 (152.6, 388.2) n = 0.7576 (0.6399, 0.8836)	1,131,543	0.9803	13
Zero-order	$F(t) = k \times t$	TA3	k = 79.2 (74.96, 83.44)	1,107,096	0.9752	14
		F10	k = 97.37 (90.95, 103.8)	2,534,552	0.9560	14
Korsmeyer-Peppas	$F(t) = k_{KP} \times t^n \times Q_0$	TA3	k_{KP} = 82.68 (42.18, 151.6) n = 0.9889 (0.8317, 1.161)	1,105,283	0.9752	13
		F10	k_{KP} = 248 (152.6, 388.2) n = 0.7576 (0.6399, 0.8836)	1,131,543	0.9803	13

of chitosan in an acid gelling bath led to an increase in the encapsulation efficiency, making the ionotropic gelation technique more advantageous for the delivery of highly soluble compounds. The chitosan, as an additional carrier-excipient, was also shown to improve the characteristics of the obtained microparticles in terms of residual humidity, morphology, and flowability. At the same time, the swelling behavior, the thermal stability, and the release ability of the polymeric structure were not significantly altered.

Overall, the data collected confirmed the possibility of applying the ionotropic gelation technique, characterized by mild process conditions and biocompatible, biodegradable, and non-toxic materials, to efficiently encapsulate highly water-soluble compounds without wasting them, keeping the same cost-effectiveness of the process.

In further studies, the ability of selected systems to preserve the active compounds for a long period will be evaluated by stability studies, and additional tests will be performed to decrease the particle size, thus expanding the possibilities of application, and evaluating if the adopted formulation strategy could be successful regardless of the particle dimensions.

CRediT authorship contribution statement

Giada Diana: Writing – original draft, Visualization, Methodology, Investigation, Formal analysis, Data curation. **Alessandro Candiani:** Writing – review & editing, Visualization, Investigation. **Alice Picco:** Writing – review & editing, Visualization, Investigation. **Andrea Milanesi:** Writing – review & editing, Visualization, Formal analysis. **Margherita Stampini:** Writing – review & editing, Investigation. **Elia Bari:** Writing – review & editing, Visualization. **Maria Luisa Torre:** Writing – review & editing, Supervision. **Lorena Segale:** Writing – original draft, Supervision, Resources, Project administration, Methodology, Data curation, Conceptualization. **Lorella Giovannelli:** Writing – review & editing, Supervision, Resources, Project administration, Methodology, Conceptualization.

Declaration of competing interest

The authors declare the following financial interests/personal relationships which may be considered as potential competing interests: Segale L., Giovannelli L. are co-founders and members of the advisory board of the company APTSol S.r.l., Milanesi A. is member of advisory board of the company APTSol S.r.l. Torre M.L. is co-founder and member of the advisory board of the company Pharmaexceed. The other authors declare that they have no known competing financial interests or personal relationships that could have appeared to influence the work reported in this paper.

References

[1] C. Tan, M. Arshadi, M.C. Lee, M. Godec, M. Azizi, B. Yan, H. Eskandarloo, T. W. Deisenroth, R.H. Darji, T. Van Pho, A. Abbaspourrad, A robust aqueous Core-Shell-Shell coconut-like nanostructure for stimuli-responsive delivery of hydrophilic cargo, ACS Nano 13 (2019) 9016–9027, https://doi.org/10.1021/acsnano.9b03049.

[2] A. Candiani, A. Milanesi, A. Foglio Bonda, G. Diana, E. Bari, L. Segale, M.L. Torre, L. Giovannelli, Solid lipid microparticles by spray congealing of water/oil emulsion: an effective/versatile loading strategy for a highly soluble drug, Pharmaceutics 14 (2022), https://doi.org/10.3390/pharmaceutics14122805.

[3] N.T.T. Uyen, Z.A.A. Hamid, N.X.T. Tram, N. Ahmad, Fabrication of alginate microspheres for drug delivery: a review, Int. J. Biol. Macromol. 153 (2020), https://doi.org/10.1016/j.ijbiomac.2019.10.233.

[4] B. Balanč, A. Kalušević, I. Drvenica, M.T. Coelho, V. Djordjević, V.D. Alves, I. Sousa, M. Moldão-Martins, V. Rakić, V. Nedović, B. Bugarski, Calcium-alginate-inulin microbeads as carriers for aqueous Carqueja extract, J. Food Sci. 81 (2016), https://doi.org/10.1111/1750-3841.13167.

[5] A. Bušić, A. Belščak-Cvitanović, A. Vojvodić Cebin, S. Karlović, V. Kovač, I. Špoljarić, G. Mršić, D. Komes, Structuring new alginate network aimed for delivery of dandelion (Taraxacum officinale L.) polyphenols using ionic gelation and new filler materials, Food Res. Int. 111 (2018), https://doi.org/10.1016/j.foodres.2018.05.034.

[6] R. Stojanovic, A. Belscak-Cvitanovic, V. Manojlovic, D. Komes, V. Nedovic, B. Bugarski, Encapsulation of thyme (Thymus serpyllum L.) aqueous extract in calcium alginate beads, J. Sci. Food Agric. 92 (2012) 685–696, https://doi.org/10.1002/jsfa.4632.
[7] N.D.A. Arriola, P.I. Chater, M. Wilcox, L. Lucini, G. Rocchetti, M. Dalmina, J.P. Pearson, R.D. de Mello Castanho Amboni, Encapsulation of stevia rebaudiana Bertoni aqueous crude extracts by ionic gelation – effects of alginate blends and gelling solutions on the polyphenolic profile, Food Chem. 275 (2019). doi:https://doi.org/10.1016/j.foodchem.2018.09.086.
[8] I.M. Savic, I.M. Savic Gajic, M.G. Milovanovic, S. Zerajic, D.G. Gajic, Optimization of ultrasound-assisted extraction and encapsulation of Antioxidants from Orange peels in alginate-chitosan microparticles, Antioxidants 11 (2022), https://doi.org/10.3390/antiox11020297.
[9] Y. Wang, C. Tan, S.M. Davachi, P. Li, P. Davidowsky, B. Yan, Development of microcapsules using chitosan and alginate via W/O emulsion for the protection of hydrophilic compounds by comparing with hydrogel beads, Int. J. Biol. Macromol. 177 (2021) 92–99, https://doi.org/10.1016/j.ijbiomac.2021.02.089.
[10] A.C. Tomé, F.A. da Silva, Alginate based encapsulation as a tool for the protection of bioactive compounds from aromatic herbs, Food Hydrocolloids for Health 2 (2022), https://doi.org/10.1016/j.fhfh.2021.100051.
[11] A. Safitri, A. Roosdiana, N. Kurnianingsih, F. Fatchiyah, E. Mayasari, R. Rachmawati, Microencapsulation of *Ruellia tuberosa* L. Aqueous Root Extracts Using Chitosan-Sodium Tripolyphosphate and Their In Vitro Biological Activities, Scientifica (Cairo) 2022 (2022). doi:https://doi.org/10.1155/2022/9522463.
[12] K. Trifković, N. Milašinović, V. Djordjević, G. Zdunić, M. Kalagasidis Krušić, Z. Knežević-Jugović, K. Šavikin, V. Nedović, B. Bugarski, Chitosan crosslinked microparticles with encapsulated polyphenols: water sorption and release properties, J. Biomater. Appl. 30 (2015), https://doi.org/10.1177/0885328215598940.
[13] K.T. Trifković, N.Z. Milašinović, V.B. Djordjević, M.T.K. Krušić, Z.D. Knežević-Jugović, V.A. Nedović, B.M. Bugarski, Chitosan microbeads for encapsulation of thyme (Thymus serpyllum L.) polyphenols, Carbohydr. Polym. 111 (2014), https://doi.org/10.1016/j.carbpol.2014.05.053.
[14] V.L. Singleton, J.A. Rossi, Colorimetry of Total Phenolics with Phosphomolybdic-Phosphotungstic acid reagents, Am. J. Enol. Vitic. 16 (1965), https://doi.org/10.5344/ajev.1965.16.3.144.
[15] A.F. Bonda, A. Candiani, M. Pertile, L. Giovannelli, L. Segale, Shellac gum/carrageenan alginate-based core–shell systems containing peppermint essential oil formulated by mixture design approach, Gels 7 (2021), https://doi.org/10.3390/gels7040162.
[16] C.A. Schneider, W.S. Rasband, K.W. Eliceiri, NIH image to ImageJ: 25 years of image analysis, Nat. Methods 9 (2012), https://doi.org/10.1038/nmeth.2089.
[17] H. Demircan, R.A. Oral, Parameters affecting calcium-alginate bead characteristics: viscosity of hydrocolloids and water solubility of core material, Int. J. Biol. Macromol. 236 (2023), https://doi.org/10.1016/j.ijbiomac.2023.124011.
[18] A. Candiani, G. Diana, M. Martoccia, F. Travaglia, L. Giovannelli, J.D. Coïsson, L. Segale, Microencapsulation of a Pickering oil/water emulsion loaded with vitamin D3, Gels 9 (2023), https://doi.org/10.3390/gels9030255.
[19] R.P. Hegde, J.L. Rheingold, S. Welch, C.T. Rhodes, Studies of powder flow using a recording powder flowmeter and measurement of the dynamic angle of repose, J. Pharm. Sci. 74 (1985), https://doi.org/10.1002/jps.2600740104.
[20] Council of Europe - EDQM, European Pharmacopoeia 11th Edition, 2023.
[21] V.P. Shah, L.J. Lesko, J. Fan, N. Fleischer, J. Handerson, H. Malinowski, M. Makary, L. Ouderkirk, S. Bay, P. Sathe, G.J.P. Singh, L. Iillman, Y. Tsong, R. I. Williams, FDA guidance for industry 1 dissolution testing of immediate release solid oral dosage forms, Dissolut. Technol. 4 (1997), https://doi.org/10.14227/DT040497P15.
[22] D. Caccavo, An overview on the mathematical modeling of hydrogels' behavior for drug delivery systems, Int. J. Pharm. 560 (2019) 175–190, https://doi.org/10.1016/j.ijpharm.2019.01.076.
[23] Z. Zorić, J. Markić, S. Pedisić, V. Bučevic-Popović, I. Generalic-Mekinić, K. Grebenar, T. Kulišić-Bilušic, Stability of rosmarinic acid in aqueous extracts from different lamiaceae species after in vitro digestion with human gastrointestinal enzymes, Food Technol. Biotechnol. 54 (2016), https://doi.org/10.17113/ftb.54.01.16.4033.
[24] M.P.A. Lim, W.L. Lee, E. Widjaja, S.C.J. Loo, One-step fabrication of core-shell structured alginate-PLGA/PLLA microparticles as a novel drug delivery system for water soluble drugs, Biomater. Sci. 1 (2013) 486–493, https://doi.org/10.1039/c3bm00175j.
[25] F. Ramazani, W. Chen, C.F. Van Nostrum, G. Storm, F. Kiessling, T. Lammers, W. E. Hennink, R.J. Kok, Strategies for encapsulation of small hydrophilic and amphiphilic drugs in PLGA microspheres: state-of-the-art and challenges, Int. J. Pharm. 499 (2016) 358–367, https://doi.org/10.1016/j.ijpharm.2016.01.020.
[26] L.E. Kurozawa, M.D. Hubinger, Hydrophilic food compounds encapsulation by ionic gelation, Curr. Opin. Food Sci. 15 (2017) 50–55, https://doi.org/10.1016/j.cofs.2017.06.004.
[27] V. Bhardwaj, G. Harit, S. Kumar, Interpenetrating polymer network (IPN): novel approach in drug delivery, International Journal of Drug Development and Research 4 (2012).
[28] P. Matricardi, C. Di Meo, T. Coviello, W.E. Hennink, F. Alhaique, Interpenetrating polymer networks polysaccharide hydrogels for drug delivery and tissue engineering, Adv. Drug Deliv. Rev. 65 (2013), https://doi.org/10.1016/j.addr.2013.04.002.
[29] K.Y. Lee, D.J. Mooney, Alginate: properties and biomedical applications, Progress in Polymer Science (Oxford) 37 (2012), https://doi.org/10.1016/j.progpolymsci.2011.06.003.
[30] G. Pasparakis, N. Bouropoulos, Swelling studies and in vitro release of verapamil from calcium alginate and calcium alginate-chitosan beads, Int. J. Pharm. 323 (2006) 34–42, https://doi.org/10.1016/j.ijpharm.2006.05.054.
[31] L. Segale, L. Giovannelli, P. Mannina, F. Pattarino, Calcium alginate and calcium alginate-chitosan beads containing celecoxib solubilized in a self-emulsifying phase, Scientifica (Cairo) 2016 (2016), https://doi.org/10.1155/2016/5062706.
[32] M. Vakarelova, F. Zanoni, G. Donà, I. Fierri, R. Chignola, S. Gorrieri, G. Zoccatelli, Microencapsulation of astaxanthin by ionic gelation: effect of different gelling polymers on the carotenoid load, stability and bioaccessibility, Int. J. Food Sci. Technol. 58 (2023) 2489–2497, https://doi.org/10.1111/ijfs.16389.
[33] E. Dobroslavić, Z. Zorić, V. Dragović-Uzelac, I. Elez Garofulić, Microencapsulation of Laurus nobilis L, Leaf Extract in Alginate-Based System via Electrostatic Extrusion, Foods 12 (2023), https://doi.org/10.3390/foods12173242.
[34] A.F. Martins, P.V.A. Bueno, E.A.M.S. Almeida, F.H.A. Rodrigues, A.F. Rubira, E. C. Muniz, Characterization of N-trimethyl chitosan/alginate complexes and curcumin release, Int. J. Biol. Macromol. 57 (2013) 174–184, https://doi.org/10.1016/j.ijbiomac.2013.03.029.
[35] S.K. Motwani, S. Chopra, S. Talegaonkar, K. Kohli, F.J. Ahmad, R.K. Khar, Chitosan-sodium alginate nanoparticles as submicroscopic reservoirs for ocular delivery: formulation, optimisation and in vitro characterisation, Eur. J. Pharm. Biopharm. 68 (2008) 513–525, https://doi.org/10.1016/j.ejpb.2007.09.009.
[36] S. Takka, A. Gürel, Evaluation of chitosan/alginate beads using experimental design: formulation and in vitro characterization, AAPS PharmSciTech 11 (2010) 460–466, https://doi.org/10.1208/s12249-010-9406-z.
[37] I.A. Boškov, I.M. Savić, N. n. Grozdanić Stanisavljević, T.D. Kundaković-Vasović, J. S. Radović Selgrad, I.M. Savić Gajić, Stabilization of Black Locust Flower Extract via Encapsulation Using Alginate and Alginate–Chitosan Microparticles, Polymers (Basel) 16 (2024). doi:https://doi.org/10.3390/polym16050688.
[38] X. Meng, F. Tian, J. Yang, C.N. He, N. Xing, F. Li, Chitosan and alginate polyelectrolyte complex membranes and their properties for wound dressing application, J. Mater. Sci. Mater. Med. 21 (2010) 1751–1759, https://doi.org/10.1007/s10856-010-3996-6.
[39] Y. Liu, C.J. Zhang, J.C. Zhao, Y. Guo, P. Zhu, D.Y. Wang, Bio-based barium alginate film: preparation, flame retardancy and thermal degradation behavior, Carbohydr. Polym. 139 (2016) 106–114, https://doi.org/10.1016/j.carbpol.2015.12.044.
[40] W. Chen, H. Cheng, L. Chen, X. Zhan, W. Xia, Synthesis, characterization, and anti-tumor properties of O-benzoylselenoglycolic chitosan, Int. J. Biol. Macromol. 193 (2021) 491–499, https://doi.org/10.1016/j.ijbiomac.2021.10.086.